Brief Definitive Report

Histone Acetylation Determines the Developmentally Regulated Accessibility for T Cell Receptor γ Gene Recombination

By Yasutoshi Agata,* Tomoya Katakai,* Sang-Kyu Ye,‡ Manabu Sugai,* Hiroyuki Gonda,* Tasuku Honjo,‡ Koichi Ikuta,‡ and Akira Shimizu*

*From the *Center for Molecular Biology and Genetics, Kyoto University, Kyoto 606-8507, Japan; and the ‡Department of Medical Chemistry, Graduate School of Medicine, Kyoto University, Kyoto 606-8501, Japan*

Abstract

Variable/diversity/joining (V[D]J) recombination of the T cell receptor (TCR) and immunoglobulin (Ig) genes is regulated by chromatin accessibility of the target locus to the recombinase in a lineage- and stage-specific manner. Histone acetylation has recently been proposed as a molecular mechanism underlying the accessibility control. Here, we investigate the role for histone acetylation in the developmentally regulated rearrangements of the mouse TCR-γ gene, wherein predominant rearrangement is switched from Vγ3 to Vγ2 gene during the fetal to adult thymocyte development. Our results indicate that histone acetylation correlates with accessibility, as histone acetylation at the fetal-type Vγ3 gene in accord with germline transcription is relatively high in fetal thymocytes, but specifically becomes low in adult thymocytes within the entirely hyperacetylated locus. Furthermore, inhibition of histone deacetylation during the development of adult bone marrow–derived thymocytes by a specific histone deacetylase inhibitor, trichostatin A, leads to elevated histone acetylation, germline transcription, cleavage, and rearrangement of the Vγ3 gene. These data demonstrate that histone acetylation functionally determines the chromatin accessibility for V(D)J recombination in vivo and that an epigenetic modification of chromatin plays a direct role in executing a developmental switch in cell fate determination.

Key words: V(D)J recombination • germline transcript • ligation-mediated PCR • chromatin immunoprecipitation • histone deacetylase

Introduction

Lymphocyte development is regulated by V(D)J recombination that assembles V, D, and J gene segments in the TCR and Ig loci. V(D)J recombination reaction is catalyzed by the common enzymatic machinery that includes recombination activating gene (RAG)-1 and RAG-2 proteins (1, 2). RAG-1 and RAG-2 recognize recombination signal sequences (RSSs) that flank all the coding gene segments and then introduce cleavages of DNA at RSSs. Lymphocyte-specific recombination is primarily ensured by the restriction of RAG-1 and RAG-2 expression to defined stages of T and B lymphoid development. However, lineage- and stage-specificity of the rearrangements is regulated by the accessibility of RSSs within chromatin to the recombinase (3–5). Recent studies revealed that the cis-acting elements within TCR and Ig loci including enhancers and promoters play crucial roles in recombination by establishing the locus- and gene segment–specific accessibility (3–5). However, the molecular nature of chromatin structural modifications responsible for accessibility has long been unknown. Acetylation of the NH_2-terminal tails of histones, the most extensively characterized modification of chromatin, has been implicated for transcriptional regulation through the alteration of chromatin structure (6, 7). Recently, acetylation of histone H3 was shown to tightly correlate with locus-wide accessibility for V(D)J recombination directed by the enhancer in vivo (8), suggesting that histone acetylation might be functionally relevant to the accessibility control.

In this report, we investigate the role for histone acetylation in the accessibility control during the physiological thymocyte development. We focused on the mouse TCR-γ gene (9, 10), wherein rearrangement of Vγ3 gene is re-

Address correspondence to Y. Agata at his present address, Dept. of Biology, University of California, San Diego, La Jolla, CA 92093-0366. Phone: 858-534-8797; Fax: 858-534-7550; E-mail: yagata@biomail.ucsd.edu

stricted to fetal stages, whereas Vγ2 recombination predominates in the adult thymus (11–13). Our data demonstrate that targeted histone deacetylation is responsible for the inhibition of Vγ3 rearrangements in adult thymocytes.

Materials and Methods

Cell Preparation, Fetal Thymic Organ Culture, and Flow Cytometry. Fetal and adult thymocytes were prepared from embryonic day 14 (E14) and E16 C57BL/6 fetuses and 4-wk-old C57BL/6 mice. $CD3^-CD4^-CD8^-CD19^-TER119^-$ thymocytes were isolated by MACS (Miltenyi Biotec) and used as $CD3^-CD4^-CD8^-$ triple negative (TN) thymocytes. We routinely obtained the population of >95% purity. Fetal thymic organ culture (FTOC) was performed as described (14, 15). Fetal liver cells of E14 C57BL/6 fetuses and adult bone marrow cells of 8-wk-old C57BL/6 mice (2×10^5 cells/lobe) were transferred into 2′-deoxyguanosine–treated E15 fetal thymic lobes from ICR mice in a hanging drop for 24 h, and then organ cultured on a floating Nucleopore polycarbonate filter (Corning) with trichostatin A (TSA; 3 ng/ml; WAKO) or equal volume of DMSO as a vehicle control. Flow cytometric analysis was performed as described (14, 15). The following monoclonal antibodies were used: FITC-conjugated anti-CD3ε (145-2C11) and anti-Vγ2 (UC3-10A6) antibodies; and PE-conjugated anti-CD3ε (145-2C11) and anti-Vγ3 (536) antibodies (BD PharMingen). Viable cells were analyzed by a FACSCalibur™ with CELLQuest™ software v3.1 (Becton Dickinson).

PCR Analysis. Genomic DNA was prepared by the standard proteinase K method (16). Fivefold serial dilutions (50, 10, and 2 ng) of fetal and adult thymocyte DNAs were prepared in 25 μg/ml sonicated pBSKS. Diluted DNA and organ-cultured thymocyte DNA (equivalent to 10^3 cells) were analyzed by PCR in 10 μl reaction with 0.25 mM dNTP, 0.5 μM each primer, 5 μg/ml sonicated pBSKS, and 0.5 U of rTaq DNA polymerase (Takara). PCR was performed for 24, 28, or 32 cycles (CD3ε, Vγ coding joints, Vγ signal joints, respectively) of 94°C, 45 s, 55°C, 120 s, and 72°C, 60 s with the following primers: CD3 G1/2 F141, 5′-TCAAAGGCCAGGACGGCTAC-3′; CD3 G1/2 R636, 5′-GCCATAGTAGGATGAAGGAG-3′; for Vγ coding joints, L2, L3 (13), and STP100 (Jγ1 [17]); for Vγ signal joints, V2S-R1, 5′-GGAGTGATTCAGGGGATTCA-3′, V3S-R1, 5′-TGACATCCTTGAACCGAGTC-3′, and J1P-F1, 5′-ACAGTTTCAACACGAGTGAG-3′. PCR products were run on a 2% agarose gel, transferred to HybondN$^+$ membrane (Amersham Pharmacia Biotech), and hybridized with ^{32}P-end-labeled oligonucleotide probe as follows: CD3 G1/2 F443, 5′-GGCCCGGATTTCCTCAGTTA-3′; for Vγ coding joints, STS1008 (Jγ1 [17]); for Vγ signal joints, V2-3′b and V3-3′b (13). All the Southern blots were analyzed and quantitated using a Bio-image Analyzer (Fujix BAS5000).

Ligation-mediated PCR. The same set of the genomic DNAs was analyzed by ligation-mediated PCR as described (18). Fetal and adult thymocyte DNA (10 ng) and organ-cultured thymocyte DNA (equivalent to 2×10^3 cells) were ligated to annealed BW linker. Ligated DNA was amplified for 12 cycles with the BW-1H primer and the following distal locus-specific primer: 3′Vγ2 3′-1, 5′-CATTCAGCAGGAAACAGTGCTAACCAG-3′; Vγ3EXT (19). The first PCR product was then amplified for 30 cycles with the following linker- and proximal locus–specific primers: for Vγ2, BW-1H5, 5′-ACCCGGGAGATCTGAATTCCACAGCA-3′, 3′Vγ2 3′-2, 5′-TGATAGCAAGATAGTCCCTGAGGCT-3′; for Vγ3, BW-1H3, 5′-ACCCGGGAGATCTGAATTCCACAGT-3′, Vγ3INT (19). PCR products were analyzed by Southern blotting using the V2-3′b and V3-3′b oligonucleotides as probes.

Reverse Transcription PCR. Total RNA was prepared using TRIzol (GIBCO BRL). Random hexamer-primed cDNA was synthesized from RNA equivalent to $2–6 \times 10^4$ cells using Moloney murine leukemia virus (MMLV) reverse-transcriptase Superscript II (GIBCO BRL) according to the manufacturer's instructions. Fivefold serial dilutions of cDNA (equivalent to 5, 1, and 0.2×10^3 cells) were amplified as in genomic PCR with the following primers: for Vγ2 germline transcript (GLT), LV2, 5′-TCTTATGCCTCTTGACATTTGG-3′, V2-3′a (13); for Vγ3 GLT, LV3, 5′-TGTCTTTGACCTGTGTTTATGG-3′, V3-3′a (13); for Jγ1 GLT, 5′Jγ1 5′-2, 5′-TAACTCCAGGGAGAACAGTG-3′, Cγ1 3′-3, 5′-GACAAAGGTATGTCCCAGTC-3′; for Jκ1 GLT, 5′Jκ1 5′-4, 5′-CAGCAGTTCTCTGTCAGAGA-3′, Cκ 3′-1, 5′-GATGGTGGGAAGATGGATAC-3′; mMyoD 10691-F1, 5′-TCTACGCACCTGGACCGCTGC-3′; mMyoD 10692-R1, 5′-CAGGAGTGCCTACGGTGGTGC-3′; CD3 RT F503, 5′-AAGCCTGTGACCCGAGGAAC-3′; CD3 RT R1111, 5′-GTGTAACAGTCGGAGGATGG-3′; glyceraldehyde 3-phosphate dehydrogenase (GAPDH)-S1, 5′-CCATCACCATCTTCCAGGAG-3′; GAPDH-AS1, 5′-CCTGCTTCACCACCTTCTTG-3′. Numbers of PCR cycle were as follows: 32 (Vγ2 and Vγ3 GLTs), 26 (Jγ1 GLT), 30 (Jκ1 GLT), 25 (MyoD), 23 (CD3ε), and 22 (GAPDH). To specifically amplify the spliced forms of cDNA, each LV2 and LV3 primer was designed to span the intron between the leader and following exons of each Vγ2 and Vγ3 gene. PCR products were analyzed by Southern blotting using the following oligonucleotide as probe: V2-3′b; V3-3′b; STS1008 (Jγ1); 5′Jκ1 5′-3, 5′-CTTTCGCCTACCCACTGCTCTG-3′; MyoD RT-R2, 5′-CGGGGCTGTCTGTGGAGATGC-3′; CD3 RT-F543, 5′-GAGGGCAAAACAAGGAGCGGC-3′; GAPDH-S2, 5′-GGAGCCAAACGGGTCATCATC-3′.

Chromatin Immunoprecipitation. Soluble chromatin was prepared from $1–2 \times 10^6$ cells fixed with formaldehyde as described (20, 21). The chromatin solution (2 ml) was precleared with 120 μl of 50% protein G-Sepharose slurry preadsorbed with 100 μg/ml sonicated salmon sperm DNA (ssDNA), then aliquoted and incubated with 4 μg of antiacetylated histone H3 antibody, 1 μl of antiacetylated histone H4 antiserum (Upstate Biotechnology), or 4 μg of normal rabbit IgG (Santa Cruz Biotechnology, Inc.) overnight. Immunoprecipitates were recovered with 20 μl of 50% protein G-Sepharose/ssDNA for 2 h, washed with the buffers as described (20), and resuspended in 200 μl of 10 mM Tris-HCl, pH 8.0, 5 mM EDTA, 0.3 M NaCl, and 0.5% SDS. The beads and an input fraction saved before preclear were incubated at 65°C for at least 6 h. DNA was purified and serial dilutions of DNA were prepared in 25 μg/ml sonicated pBSKS and amplified as in genomic PCR for 28 cycles of 94°C, 20 s, 55°C, 60 s, and 72°C, 60 s with 2 s increment per each cycle using the following primers: V2P-F1, 5′-GCTCAGAACAGCTACTCTTC-3′; V2P-R1, 5′-GGATTCTCATCTGCCAGGTT-3′; V2S-F1, 5′-TTGGAGGAAGAAGACGAAGC-3′; V2S-R1, 5′-GGAGTGATTCAGGGGATTCA-3′; V3P-F1, 5′-AACAGCTCAGAAATAAGTCT-3′; V3P-R1, 5′-CTCAGGACACAAAAATAACG-3′; V3S-F2, 5′-CCACGTACTACTGTGCCTGC-3′; V3S-R1, 5′-TGACATCCTTGAACCGAGTC-3′; Jγ1 5′-2, 5′-TAGCTCAGGTTTTCACAAGG-3′; 3′Jγ1 3′-1, 5′-TCTGGAGGGAAGAAGCAATC-3′; 5′Jκ1 5′-4, 5′-CAGCAGTTCTCTGTCAGAGA-3′; 3′Jκ1 3′-1, 5′-ACAGACATAGACAACGGAAG-3′; MyoD-F1, 5′-CGCCCTACTACAC-

TCCTATTG-3′; MyoD-R1, 5′-AAGGTTCTGTGGGTTGGAATG-3′; CD3 G1/2 F443, 5′-GGCCCGGATTTCCTCAGTTA-3′; CD3 G1/2 R636, 5′-GCCATAGTAGGATGAAGGAG-3′. PCR products were analyzed by Southern blotting using the following oligonucleotide as probe: V2P-F2, 5′-TGGAAGGCGGGAGGATGAGGA-3′; V2-3′b (for V2S); V3P-F2, 5′-CTTCCTCCCCTGGCCCTTTGC-3′; V3-3′b (for V3S); 3′Jγ1 3′-3, 5′-GACTCAGGCTAAGAATATTGTAGT-3′; 5′Jκ1 5′-3, 5′-CTTTCGCCTACCCACTGCTCTG-3′; MyoD-F621, 5′-GCCAGGACGCCCCAGGACACG-3′; CD3-F557, 5′-CCTGCCTCCCCTGTCTGCTTC-3′. Southern blots were quantitated using a Bio-image Analyzer. Quantitative analysis was confirmed by comparing the dilution series. To calculate the relative histone acetylation levels, a mean value of the serial dilutions was calculated for the input (I) and immunoprecipitated (P) fractions after adjusting by the dilution factors. The P/I ratio of each locus was then compared with that of the positive control CD3ε locus.

Results and Discussion

Histone Acetylation at Vγ Genes Correlates with Accessibility during Fetal to Adult Thymocyte Development. To investigate the accessibility control of the TCR-γ gene rearrangement during the thymocyte development, we first assessed the accessibility of unrearranged Vγ2 and Vγ3 genes by measuring their germline transcripts in fetal and adult thymocytes by reverse transcription (RT)-PCR (Fig. 1, A and B). For adult thymocytes, we analyzed $CD3^-CD4^-CD8^-$ TN thymocytes, in which TCR-γ gene rearrangements take place. E14 thymocytes expressed both germline transcripts at high levels. In E16 thymocytes, Vγ3 germline transcripts began to decline by threefold compared with E14, whereas Vγ2 germline transcripts remained comparable. In contrast, germline transcripts as well as rearrangements of Vγ3 dramatically decreased in adult TN thymocytes, whereas those of Vγ2 were still predominant (Figs. 1 B and 2 B). These results confirm the previous findings that chromatin at Vγ3 is inaccessible and Vγ3 rearrangements are consequently inhibited in adult thymocytes (13). Unrearranged Jγ1 gene and CD3ε gene were vigorously transcribed in both fetal and adult thymocytes, whereas Jκ1 and MyoD were not (Fig. 1 B).

We next examined whether histone acetylation at Vγ genes correlates with accessibility. Histone acetylation was measured by chromatin immunoprecipitation (ChIP) assay (20, 21) using antiacetylated histone H3 and H4 antibodies. Immunoprecipitated DNA was analyzed by quantitative PCR to assess the association of specific DNA regions with

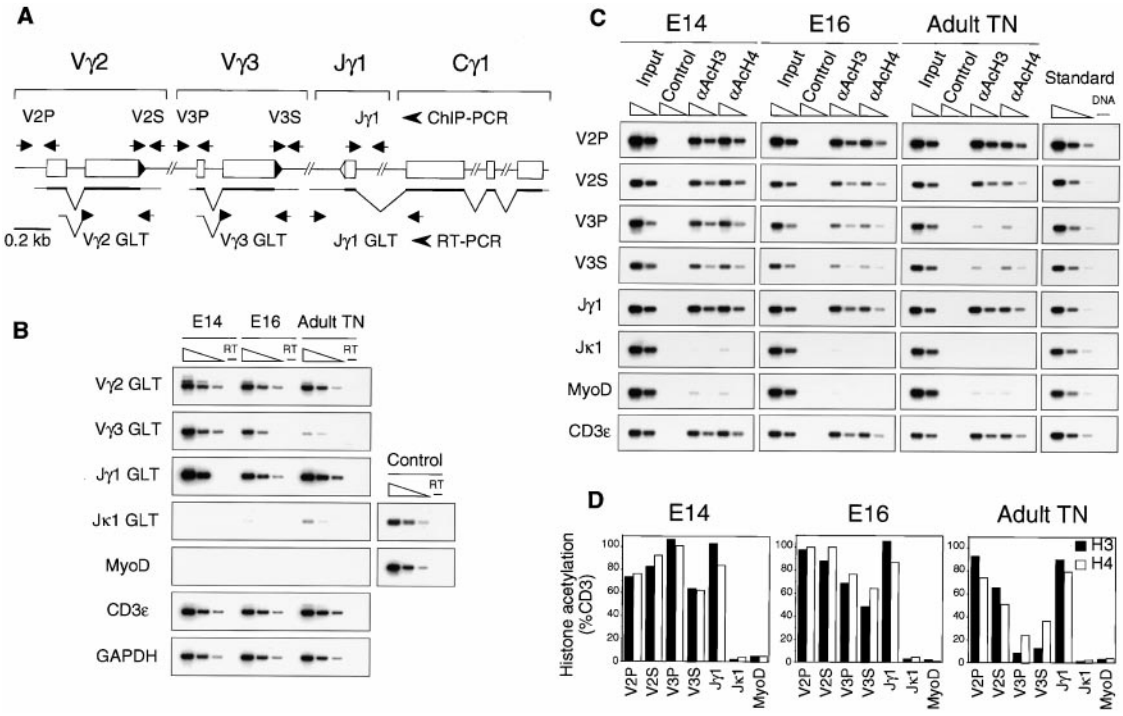

Figure 1. Histone acetylation at Vγ genes correlates with accessibility during fetal to adult thymocyte development. (A) Schematic diagram of the TCR-γ locus and location of PCR primers used in RT-PCR and ChIP assays. The promoter (P) and RSS (S) regions of each Vγ2 and Vγ3 gene were analyzed in ChIP assays. GLTs of Vγ2, Vγ3, and Jγ1 genes were measured by RT-PCR. The Vγ RSSs with 23-bp spacer and Jγ1 RSS with 12-bp spacer are indicated by filled and open triangles. (B) RT-PCR analysis of E14 and E16 total, and adult $CD3^-CD4^-CD8^-$ TN thymocyte RNA. Fivefold serial dilutions of cDNAs and reaction without reverse transcriptase (RT−) were amplified for indicated transcripts. For Jκ1 GLT and MyoD transcripts, cDNAs from adult bone marrow and C2C12 cells were used, respectively (Control). (C) Histone acetylation measured by ChIP assay in E14 and E16 total, and adult TN thymocytes. Threefold serial dilutions of input DNA and DNAs immunoprecipitated with antiacetylated histone H3 (αAcH3) and H4 (αAcH4) antibodies or with normal rabbit IgG (Control) were analyzed by PCR. Fivefold serial dilutions of input DNA from Ba/F3 cells (Standard) and no DNA control (DNA−) were also subjected to PCR. (D) Histone acetylation levels measured in C are shown as relative histone H3 (black bars) and H4 (white bars) acetylation levels to that of the CD3ε locus.

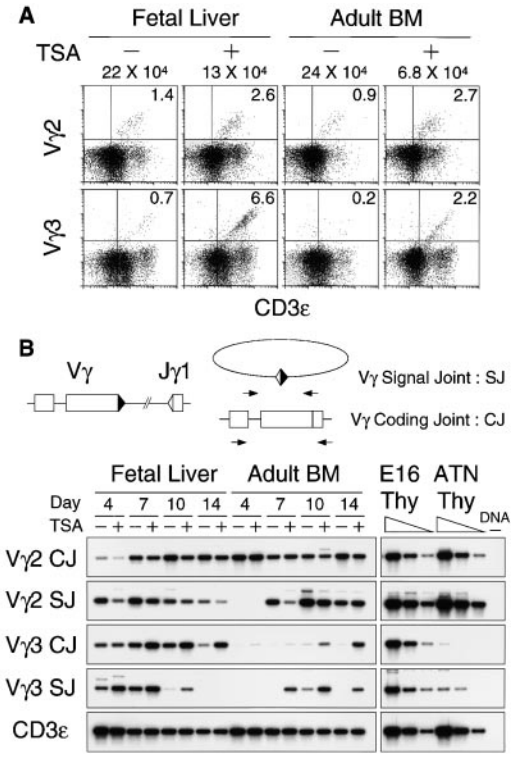

Figure 2. TSA induces Vγ3 rearrangements in adult-derived thymocytes. (A) Flow cytometric analysis of organ-cultured thymocytes in fetal thymic lobes repopulated with E14 fetal liver and adult bone marrow (BM) cells. Thymocytes cultured for 14 d with (+) or without (−) TSA were stained with FITC-Vγ2 and PE-CD3ε, or PE-Vγ3 and FITC-CD3ε antibodies. Average cell numbers per lobe from four lobes and percentages of cells for a given phenotype are shown above and inside each panel, respectively. (B) PCR analysis of organ-cultured thymocyte DNA to measure coding joints (CJ) and signal joints (SJ) of Vγ2-Jγ1 or Vγ3-Jγ1, and CD3ε gene for a control. Fivefold serial dilutions of E16 and adult TN (ATN) thymocyte (Thy) DNA and no DNA control (DNA−) were also subjected to PCR.

acetylated histones. We examined two regions corresponding to the promoter and RSS for each Vγ gene (Fig. 1 A). Histone acetylation at the promoters may reflect transcription on productively rearranged alleles. On the other hand, PCR products of RSS regions that are deleted by recombination reflect the acetylation state before recombination. To compensate deletions by recombination, histone acetylation levels were normalized with input DNA, and then compared with that of the positive control CD3ε locus. Consistent with abundant germline transcripts, we detected high levels of histone H3 and H4 acetylation at Vγ2, Vγ3, and Jγ1 in E14 thymocytes, whereas acetylation levels were extremely low at Jκ1 and MyoD (Fig. 1, C and D). We reproducibly observed that acetylation at Vγ3 promoter was slightly higher than that of Vγ2 promoter (Fig. 1 D). In E16 thymocytes, the acetylation pattern at promoters became opposite, whereas that of RSSs was unchanged (Fig. 1 D), indicating that histone acetylation at Vγ3 promoter correlates well with germline transcription during fetal stages. Nevertheless, general acetylation levels in the promoter and RSS regions are relatively high at both Vγ2 and Vγ3. In contrast, acetylation levels at Vγ3 promoter and RSS specifically decreased in adult TN thymocytes, whereas those at Vγ2 and Jγ1 remained relatively high (Fig. 1 D). It might be argued that the decreased levels of histone acetylation and germline transcription at Vγ3 in adult TN thymocytes are due to excision out of Vγ3 gene by the rearrangements of Vγ2 (or Vγ4) to Jγ1. However, we confirmed by Southern blotting that extrachromosomal species were estimated to be less than one-third of Vγ3 gene in adult TN thymocytes (data not shown). Thus, reduced histone acetylation and germline transcription at Vγ3 that we detected were not solely attributed to the excision. Furthermore, similar reduction was also found in adult thymocytes of RAG-2 knockout mouse (data not shown). These results indicate that histone acetylation is tightly correlated with germline transcription and hence accessibility on the chromosomal Vγ3 gene during fetal to adult thymocyte development. These data led us to the hypothesis that histone deacetylation at Vγ3 may play a role in establishment and maintenance of the inaccessible chromatin structure of Vγ3 gene in adult thymocytes.

Inhibition of Histone Deacetylase Induces Vγ3 Rearrangements in Adult-derived Thymocytes. To address this hypothesis, we tested whether inhibition of histone deacetylation by TSA (22) affects development of $V\gamma3^+$ T cells in FTOC (Fig. 2 A). E14 fetal liver and adult bone marrow cells were transferred into 2′-deoxyguanosine–treated fetal thymic lobes and then cultured with or without TSA. After 14 d, thymocytes were prepared from the cultured lobes and analyzed by flow cytometry. Both fetal liver and adult bone marrow cells gave rise to $V\gamma2^+$ T cells irrespective of TSA treatment. In contrast, a small but discrete $V\gamma3^+$ T cell population was detected in fetal- but not adult-derived thymocytes without TSA, confirming our previous finding that the potential to differentiate into $V\gamma3^+$ T cells is determined at the stem cell level (14). However, in the presence of TSA both fetal liver and adult bone marrow cells gave rise to distinct $V\gamma3^+$ populations. This is not due to relative enrichment because the absolute numbers of $V\gamma3^+$ cells, but not of $V\gamma2^+$ cells, were significantly increased by TSA. These data indicate that TSA treatment promotes development of fetal-type $V\gamma3^+$ T cells. We also verified the donor origin of $V\gamma3^+$ cells by allotypic marker (CD45.1 and CD45.2) staining (data not shown).

To determine whether Vγ3 rearrangements are also promoted by TSA, we next analyzed organ-cultured thymocyte DNA to quantitate coding joints between Vγ and Jγ1 exons by PCR (Fig. 2 B). Vγ2 coding joints were readily detected in both fetal- and adult-derived thymocytes. Vγ3 coding joints were also detected in fetal-derived cells, but barely detectable in adult-derived cells without TSA (Fig. 2 B, TSA^- lanes). By TSA treatment, however, Vγ3 but not Vγ2 coding joints were significantly increased in adult-derived cells (5- and 17-fold on day 10 and 14, respectively, compare TSA + to − lanes in Fig. 2 B). In fetal-derived cells, TSA also increased Vγ3 coding joints sevenfold on day 14, but did not significantly affect them until day 10. Consistent with the data in the flow cytometric analysis, these results

suggest that inhibition of histone deacetylation by TSA leads either to specific induction of Vγ3 recombination or to selective expansion of Vγ3-rearranged cells.

To discriminate these two possibilities, we examined reciprocal Vγ-Jγ1 signal joints that are recombination byproducts generated by joining between Vγ and Jγ1 RSSs (Fig. 2 B). The amount of signal joints usually reflects de novo recombination events, because they are present on circular DNAs that do not replicate in most cases. Vγ3 but not Vγ2 signal joints were specifically reduced in adult TN thymocytes as well as adult-derived thymocytes without TSA (Fig. 2 B, TSA^- lanes). However, TSA strongly increased Vγ3 signal joints in adult-derived cells (Fig. 2 B, compare TSA + to − lanes). A small amount of Vγ3 signal joints was detected on day 10 without TSA, but was increased sevenfold by TSA. These results demonstrate that de novo Vγ3-Jγ1 recombination is induced by TSA in adult-derived thymocytes. In addition, TSA-induced recombination apparently included productive Vγ3-Jγ1 recombination, as revealed by the flow cytometric analysis (Fig. 2 A). However, it should be noted that expansion of Vγ3-rearranged cells partially contributed to the increased Vγ3 coding joints from day 10 to 14 in adult-derived cells cultured with TSA because Vγ3 signal joints reciprocally decreased (Fig. 2 B). In fetal-derived thymocytes, high levels of Vγ3 coding and signal joints were detected until day 7 irrespective of TSA treatment, and then signal joints were rapidly decreased and coding joints were also gradually reduced without TSA. However, TSA treatment maintained high levels of Vγ3 coding joints up to day 14 despite the rapid loss of signal joints, indicating that TSA prolonged the growth of Vγ3-rearranged cells. This explains the apparent increase of $V\gamma3^+$ population in fetal-derived thymocytes detected by the flow cytometric analysis (Fig. 2 A).

Accessibility at Vγ3 Is Increased by TSA in Adult-derived Thymocytes. VDJ recombination is initiated by cleavages at RSSs. We thus assessed whether TSA induces cleavages at Vγ3 RSS in adult-derived thymocytes. To this end, we analyzed Vγ signal broken ends (SBEs) in organ-cultured thymocytes by ligation-mediated PCR (18, 23; Fig. 3 A). SBEs are recombination intermediates produced on cleavage at RSSs by the RAG proteins, which directly reflect the accessibility of RSSs (1, 2). Both Vγ2 and Vγ3 SBEs were detected in E16 and fetal liver–derived thymocytes. In contrast, Vγ3 SBEs were hardly detectable in adult TN thymocytes and adult-derived thymocytes without TSA, whereas Vγ2 SBEs were readily detected. By TSA treatment, however, Vγ3 SBEs were strongly induced in adult-derived cells. This is not due to accumulation by inhibiting joining process because the signal joints were concomitantly increased (Fig. 2 B). These results demonstrate that TSA treatment induces initiation of the recombination event by increasing the accessibility at Vγ3 RSS in adult-derived thymocytes.

To further confirm the TSA-induced accessibility of Vγ3 chromatin, we also analyzed germline transcripts of Vγ genes in organ-cultured thymocytes by RT-PCR (Fig. 3 B). Vγ3 but not Vγ2 germline transcripts were specifically reduced in adult-derived cells cultured for 7 d without TSA by threefold compared with fetal-derived cells. TSA treatment augmented Vγ3 germline transcript level three- to fourfold. Kinetic analysis clearly showed three- to fourfold enhancement of Vγ3 germline transcription by TSA from day 7 to 14 in adult-derived cells (Fig. 3 C). This is in good agreement with the kinetics of Vγ3 SBEs (Fig. 3 A). Vγ2 germline transcripts also increased in parallel with SBEs from day 7 to 10 irrespective of TSA treatment, although TSA slightly enhanced germline transcription (Fig. 3 C). In striking contrast to adult-derived cells, fetal-derived thymocytes exhibited prominent germline transcripts and SBEs of both Vγ genes in the early phase of culture (Fig. 3, A and C), indicating that chromatin is accessible at both Vγ genes in fetal-derived cells. These data demonstrate that TSA specifically alters Vγ3 chromatin from inaccessible to accessible state in adult-derived thymocytes.

Histone Acetylation at Vγ3 Is Increased by TSA in Adult-derived Thymocytes. If TSA induces accessibility by directly increasing histone acetylation, the acetylation level at Vγ3 should be elevated by TSA treatment. To confirm this, we

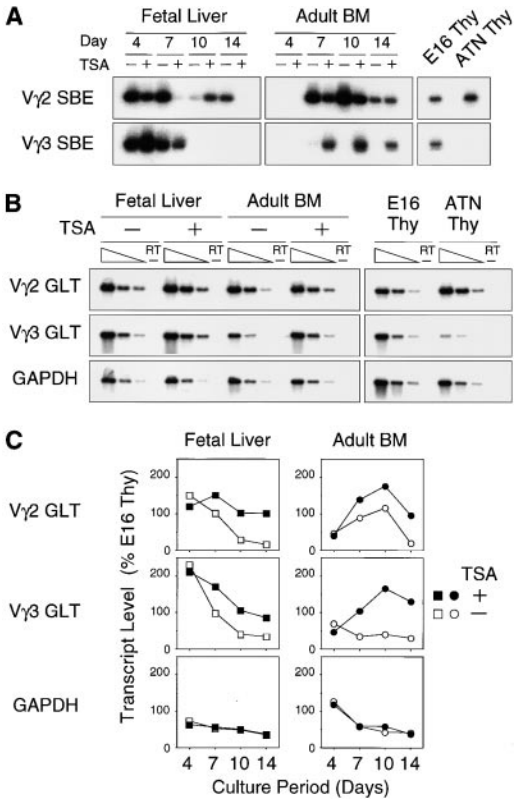

Figure 3. Accessibility at Vγ3 is increased by TSA in adult-derived thymocytes. (A) Ligation-mediated PCR analysis of organ-cultured thymocyte DNA used in Fig. 2 B to measure SBEs at Vγ2 and Vγ3. (B) RT-PCR analysis of RNA prepared from fetal liver- and adult bone marrow (BM)-derived thymocytes cultured for 7 d with (+) or without (−) TSA, and from E16 and adult TN (ATN) thymocytes (Thy). Fivefold serial dilutions of cDNAs and reaction without reverse transcriptase (RT−) were amplified for Vγ2, Vγ3 GLTs, and GAPDH transcripts. (C) Kinetic analysis of transcript levels in organ-cultured thymocytes. Transcript levels measured as in B are shown as the ratio to those in E16 thymocytes.

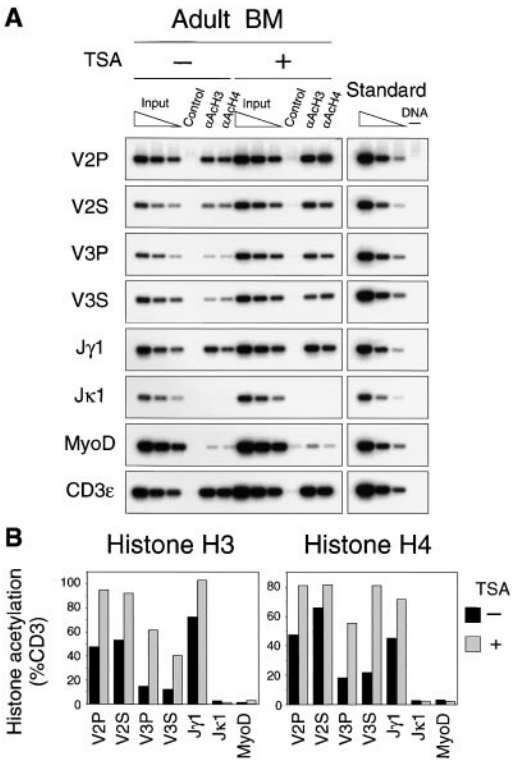

Figure 4. Histone acetylation at Vγ3 is increased by TSA in adult-derived thymocytes. (A) Histone acetylation measured by ChIP assay in adult bone marrow (BM)-derived thymocytes cultured for 15 days with (+) or without (−) TSA. ChIP and PCR analysis were performed as in the legend to Fig. 1 except that twofold serial dilutions of input DNA were amplified. (B) Histone acetylation levels in thymocytes cultured with (shaded bars) or without (black bars) TSA measured in A are shown as relative histone acetylation levels to that of the CD3ε locus.

assessed histone acetylation of Vγ3 chromatin in organ-cultured thymocytes by ChIP assay (Fig. 4). Adult bone marrow–derived thymocytes cultured without TSA showed low levels of histone H3 and H4 acetylation at Vγ3, whereas modest acetylation could be detected at Vγ2 and Jγ1. TSA increased acetylation of both histone H3 and H4 at Vγ3 by three- to fourfold. Acetylation levels at Vγ2 and Jγ1 were slightly elevated, suggesting that TSA affects histone acetylation along the entire TCR-γ locus. Nevertheless, the most striking effect was observed at Vγ3, consistent with the specific enhancement of cleavage and germline transcription at Vγ3. Although elevated acetylation at Vγ3 promoter may simply reflect the increased Vγ3 rearrangements, similar enhancement was observed for acetylation at Vγ3 RSS as well as Vγ3 germline transcription that were derived from unrearranged alleles. These data collectively indicate that TSA indeed increases histone acetylation and accessibility of Vγ3 chromatin, thereby inducing Vγ3 rearrangements in adult bone marrow–derived thymocytes.

The accessibility model for V(D)J recombination predicts that specific modifications of chromatin at RSSs regulate cleavage by RAG proteins in a lineage- and stage-specific manner (3–5). Recent biochemical studies revealed that packaging of RSSs into mononucleosomes severely inhibited cleavage in vitro (24, 25) and that histone acetylation did not stimulate cleavage (25) despite the functional involvement of histone acetylation was suggested in the accessibility control in vivo (8). Thus, it has been postulated that histone acetylation may regulate accessibility in vivo depending on the higher order chromatin structures or chromatin remodeling activities that are not reproduced in vitro (8). We demonstrate here that inhibition of histone deacetylation leads to elevated histone acetylation, accessibility, and rearrangement of the Vγ3 gene. Our data thus provide evidence that histone acetylation is the chromatin modification that triggers all the in vivo processes that induce accessibility, possibly including chromatin remodeling. During the preparation of our manuscript, several studies supporting our conclusion have been reported. Histone deacetylase inhibition by TSA also stimulated V(D)J recombination in cultured cell line (26) and thymocytes of the TCR-β enhancer-deleted mice (27). Moreover, hSWI/SNF-mediated chromatin remodeling was shown to act in concert with histone acetylation to stimulate cleavage on mononucleosomal DNA (28).

What is the mechanism underlying differential acetylation and accessibility in the Vγ regions? The entire TCR-γ locus is hyperacetylated and accessible in fetal thymocytes, whereas Vγ3 chromatin specifically becomes hypoacetylated and inaccessible in adult thymocytes. Inhibition of histone deacetylation by TSA increased transcription and accessibility at Vγ3, despite the fact that TSA does not cause the widespread gene activation (29). These data can not be attributed to the selective loss of factors inducing accessibility at Vγ3 in adult thymocytes. Rather, they strongly suggest that an active mechanism must exist to reduce the localized accessibility at Vγ3. This idea is consistent with the previous report that the Vγ3 upstream sequence, when swapped with the Vγ2 upstream sequence in transgenes, reduced rearrangements of the Vγ2 gene in adult thymocytes (30). A specific factor may bind to the Vγ3 upstream sequence and recruit a histone deacetylase activity, which reduces histone acetylation and accessibility at Vγ3 chromatin. Once established, such inaccessible chromatin probably plays a dominant role over the factors inducing accessibility. Thus, our data imply that establishment of inaccessible chromatin by targeted histone deacetylation may also serve as an active and dynamic mechanism for other developmentally regulated processes such as allelic exclusion in the Ig heavy chain and TCR-β loci.

We thank Drs. T. Kina, K. Kuroda, H. Kurooka, K. Maki, E. Matsuda, C. Murre, W.J. Romanow, and Y. Yokota for materials and discussion; and Ms. S. Hirano, M. Tanaka, T. Taniuchi, Y. Tabuchi, T. Toyoshima, and S. Nomura for their technical assistance.

This work was supported in part by Grants-in-Aid from the Ministry of Education, Science, Sports, and Culture of Japan.

Submitted: 6 December 2000
Revised: 16 January 2001
Accepted: 24 January 2001

References

1. Gellert, M. 1997. Recent advances in understanding V(D)J recombination. *Adv. Immunol.* 64:39–64.
2. Schatz, D.G. 1997. V(D)J recombination moves in vitro. *Semin. Immunol.* 9:149–159.
3. Sleckman, B.P., J.R. Gorman, and F.W. Alt. 1996. Accessibility control of antigen-receptor variable-region gene assembly: role of cis-acting elements. *Annu. Rev. Immunol.* 14:459–481.
4. Schlissel, M.S., and P. Stanhope-Baker. 1997. Accessibility and the developmental regulation of V(D)J recombination. *Semin. Immunol.* 9:161–170.
5. Hempel, W.M., I. Leduc, N. Mathieu, R.K. Tripathi, and P. Ferrier. 1998. Accessibility control of V(D)J recombination: lessons from gene targeting. *Adv. Immunol.* 69:309–352.
6. Struhl, K. 1998. Histone acetylation and transcriptional regulatory mechanisms. *Genes Dev.* 12:599–606.
7. Workman, J.L., and R.E. Kingston. 1998. Alteration of nucleosome structure as a mechanism of transcriptional regulation. *Annu. Rev. Biochem.* 67:545–579.
8. McMurry, M.T., and M.S. Krangel. 2000. A role for histone acetylation in the developmental regulation of VDJ recombination. *Science.* 287:495–498.
9. Raulet, D.H. 1989. The structure, function, and molecular genetics of the gamma/delta T cell receptor. *Annu. Rev. Immunol.* 7:175–207.
10. Raulet, D.H., D.M. Spencer, Y.H. Hsiang, J.P. Goldman, M. Bix, N.S. Liao, M. Zijstra, R. Jaenisch, and I. Correa. 1991. Control of gamma delta T-cell development. *Immunol. Rev.* 120:185–204.
11. Garman, R.D., P.J. Doherty, and D.H. Raulet. 1986. Diversity, rearrangement, and expression of murine T cell gamma genes. *Cell.* 45:733–742.
12. Heilig, J.S., and S. Tonegawa. 1986. Diversity of murine gamma genes and expression in fetal and adult T lymphocytes. *Nature.* 322:836–840.
13. Goldman, J.P., D.M. Spencer, and D.H. Raulet. 1993. Ordered rearrangement of variable region genes of the T cell receptor gamma locus correlates with transcription of the unrearranged genes. *J. Exp. Med.* 177:729–739.
14. Ikuta, K., T. Kina, I. MacNeil, N. Uchida, B. Peault, Y.H. Chien, and I.L. Weissman. 1990. A developmental switch in thymic lymphocyte maturation potential occurs at the level of hematopoietic stem cells. *Cell.* 62:863–874.
15. Ye, S.K., K. Maki, T. Kitamura, S. Sunaga, K. Akashi, J. Domen, I.L. Weissman, T. Honjo, and K. Ikuta. 1999. Induction of germline transcription in the TCRgamma locus by Stat5: implications for accessibility control by the IL-7 receptor. *Immunity.* 11:213–223.
16. Ausubel, F., R. Brent, R. Kingston, D. Moore, J. Seidman, J. Smith, and K. Struhl. 1987. Current Protocols in Molecular Biology. Wiley-Interscience, J. Wiley & Sons, New York.
17. Itohara, S., P. Mombaerts, J. Lafaille, J. Iacomini, A. Nelson, A.R. Clarke, M.L. Hooper, A. Farr, and S. Tonegawa. 1993. T cell receptor delta gene mutant mice: independent generation of alpha beta T cells and programmed rearrangements of gamma delta TCR genes. *Cell.* 72:337–348.
18. Schlissel, M., A. Constantinescu, T. Morrow, M. Baxter, and A. Peng. 1993. Double-strand signal sequence breaks in V(D)J recombination are blunt, 5′-phosphorylated, RAG-dependent, and cell cycle regulated. *Genes Dev.* 7:2520–2532.
19. Bain, G., W.J. Romanow, K. Albers, W.L. Havran, and C. Murre. 1999. Positive and negative regulation of V(D)J recombination by the E2A proteins. *J. Exp. Med.* 189:289–300.
20. Braunstein, M., A.B. Rose, S.G. Holmes, C.D. Allis, and J.R. Broach. 1993. Transcriptional silencing in yeast is associated with reduced nucleosome acetylation. *Genes Dev.* 7:592–604.
21. Orlando, V., H. Strutt, and R. Paro. 1997. Analysis of chromatin structure by in vivo formaldehyde cross-linking. *Methods.* 11:205–214.
22. Yoshida, M., S. Horinouchi, and T. Beppu. 1995. Trichostatin A and trapoxin: novel chemical probes for the role of histone acetylation in chromatin structure and function. *Bioessays.* 17:423–430.
23. Roth, D.B., C. Zhu, and M. Gellert. 1993. Characterization of broken DNA molecules associated with V(D)J recombination. *Proc. Natl. Acad. Sci. USA.* 90:10788–10792.
24. Kwon, J., A.N. Imbalzano, A. Matthews, and M.A. Oettinger. 1998. Accessibility of nucleosomal DNA to V(D)J cleavage is modulated by RSS positioning and HMG1. *Mol. Cell.* 2:829–839.
25. Golding, A., S. Chandler, E. Ballestar, A.P. Wolffe, and M.S. Schlissel. 1999. Nucleosome structure completely inhibits in vitro cleavage by the V(D)J recombinase. *EMBO (Eur. Mol. Biol. Organ.) J.* 18:3712–3723.
26. McBlane, F., and J. Boyes. 2000. Stimulation of V(D)J recombination by histone acetylation. *Curr. Biol.* 10:483–486.
27. Mathieu, N., W.M. Hempel, S. Spicuglia, C. Verthuy, and P. Ferrier. 2000. Chromatin remodeling by the T cell receptor (TCR)-beta gene enhancer during early T cell development: Implications for the control of TCR-beta locus recombination. *J. Exp. Med.* 192:625–636.
28. Kwon, J., K.B. Morshead, J.R. Guyon, R.E. Kingston, and M.A. Oettinger. 2000. Histone acetylation and hSWI/SNF remodeling act in concert to V(D)J cleavage of nucleosomal. *Mol. Cell.* 6:1037–1048.
29. Van Lint, C., S. Emiliani, and E. Verdin. 1996. The expression of a small fraction of cellular genes is changed in response to histone hyperacetylation. *Gene Expr.* 5:245–253.
30. Baker, J.E., D. Cado, and D.H. Raulet. 1998. Developmentally programmed rearrangement of T cell receptor Vgamma genes is controlled by sequences immediately upstream of the Vgamma genes. *Immunity.* 9:159–168.